



Product Description Document (PDD)

X-band Radar dataset

Contributors: Lohitzune Solabarrieta, Ivan Manso-Narvarte, Alexandre Clot, Ainhoa Caballero.

Version	Changes made by	Nature of changes
V_2023_08	L. Solabarrieta, I. Manso-Narvarte A. Caballero, J.A. Fernandes-Salvador	Document generation

1 Introduction

X-band (low-range) navigational radars can be used as active oceanographic remote sensing devices operating in the microwave range. These platforms are designed to monitor processes with high spatio-temporal resolution and can complement other remote (satellites, high-frequency radars) or in situ platforms (buoys, fixed platforms). The obtained data could contribute to global data portals in different ways, e.g. as in situ datasets or for assimilation into models.

This section describes surface currents and wave datasets, built in the framework of the SusTunTech project, collected between 2021 and 2023 in two coastal sites in the south-eastern Bay of Biscay: Biarritz (France) and Bilbao (Spain).

2 Data provenance

The X-band radar relies on the backscattering of the electromagnetic waves on the ripple waves of the sea surface, which modulate the received image. Several studies have been conducted and published regarding the most common processing of raw X-band radar images, based on spectral analysis. The reader is referred to Valenzuela (1978), Young *et al.* (1985), Nieto Borge *et al.* (2004) and Serafino *et al.* (2008).

The X-band radar data were obtained at two different sites. The first onsite installation was done on the top of the Casino building in Biarritz, France (Figure 1) and the second one in Bilbao Harbor, Basque Country, Spain, over a metallic structure at 12m height (Figure 2).



Figure 1. X-band radar installed on the top of the Casino in Biarritz.



Figure 2. X-band radar installed on the top of the breakwater, in Bilbao Port.

The testing installation in Biarritz successfully provided hourly surface current velocity and wave data, from March 2021 to February 2022 of the area covered by the X-band radar, i.e. from the coastline up to 3 km offshore. The second installation also provided hourly surface current velocity and wave data, from November 2022 to April 2023. The areas monitored by the Biarritz and Bilbao installation are shown in Figure 3 (left) and Figure 3 (right), respectively.

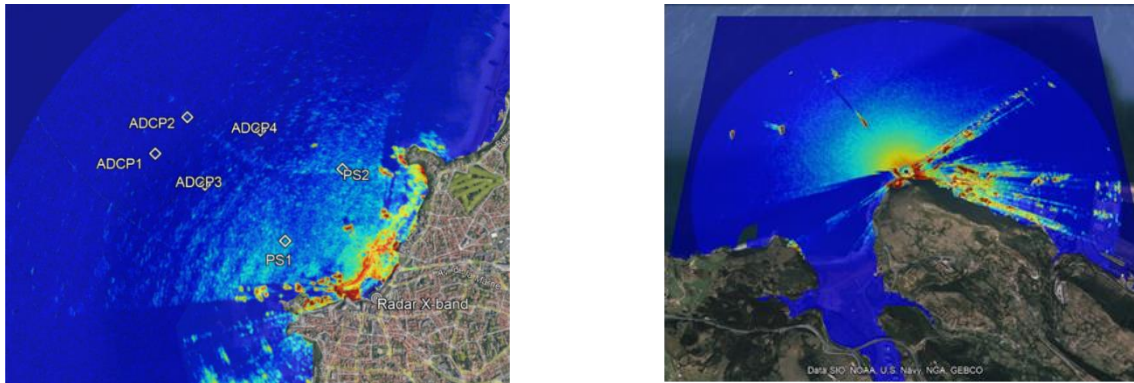


Figure 3. Areas covered by the X-band radar installed (left) on the top of the Casino in Biarritz and (right) on the top of the Breakwater in Bilbao Port.

The specific low-range radar observation system used for the data collection is made up of the following elements (Figure 4):

- 1 Radar Unit (box of 0.3 m x 0.3 m x 0.3 m and 30 kg).
- 1 Antenna (2.1 m wide swivel and 7 kg)
- 1 PC tower (15 kg)
- 1 Radar power supply (2 small boxes of 0.2 m x 0.4 m x 0.1 m, 3 kg)



Figure 4. X-band marine radar (low range) provided by the HZG Institute, Germany.

The main characteristics of this X-band radar are summarized in Table 1.

Table 1. Main characteristics of the X-band radar.

Peak Power (nominal)	12 kW
Transmit frequency	9410 \pm 30 MHz
Pulse width	60 \pm 20 ns
Pulse repetition frequency	2 or 1 kHz \pm 5 Hz tolerance
Intermediate frequency	60 \pm 2 MHz
Intermediate frequency bandwidth	20 MHz with \pm 10% tolerance
Noise Figure (radar front end)	Nominal 3.5 dB
Antenna rotation speed	up to 36 rpm
Linear amplification	30 to 40 dB
Digitization frequency	80 MHz, 2 channel with 14 bit
Antenna Length	7.5'
Horizontal beamwidth	1.2° \pm 0.1°
Vertical beamwidth	22° \pm 2°
Sidelobes within \pm 10°	-25 dB
Sidelobes outside \pm 10°	-30 dB
Gain	\geq 30 dBi

3 Dataset description

The surface currents and waves data were obtained from the two installations of the X-band radar system described in the previous section, covering these periods:

- Biarritz: March 2021 -February 2022
- Bilbao port: November 2022- April 2023.

This system was configured to measure 20 minutes every hour, from HH:00 to HH:20. The radar software converts the raw spectral data into surface currents and waves direction, wave magnitude and wave period. The software used in this processing is the Radar Ocean Waves Monitoring System (ROWMS), developed by the team from the Helmholtz-Zentrum Hereon (Seemann *et al.*, 2017). This processing can be done in Near Real Time (NRT) or post-processed.

An example of surface West-East/North-South currents and wave parameters retrieved in NRT during 2021-2023 in the Biarritz and Bilbao installations are shown in Figures 5 to 8.

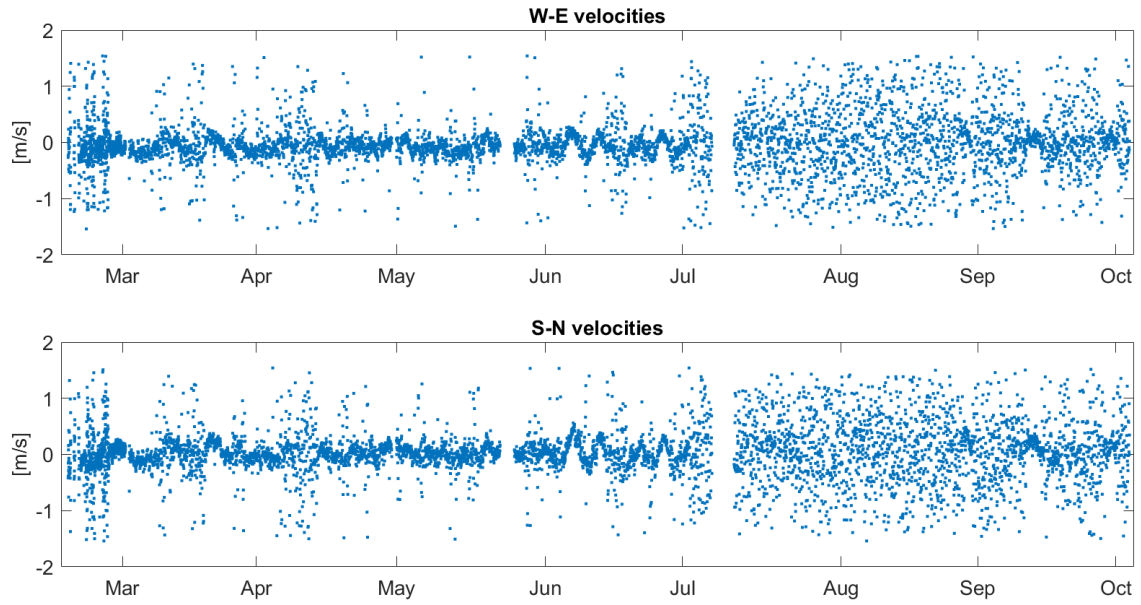


Figure 5. West-East and South-North currents extracted from X-band radar data in NRT processing, during the Biarritz testing period. Note: data values shown are directly retrieved from the X-band radar and a validation and QC process is required to identify and discard (if needed) bad data.

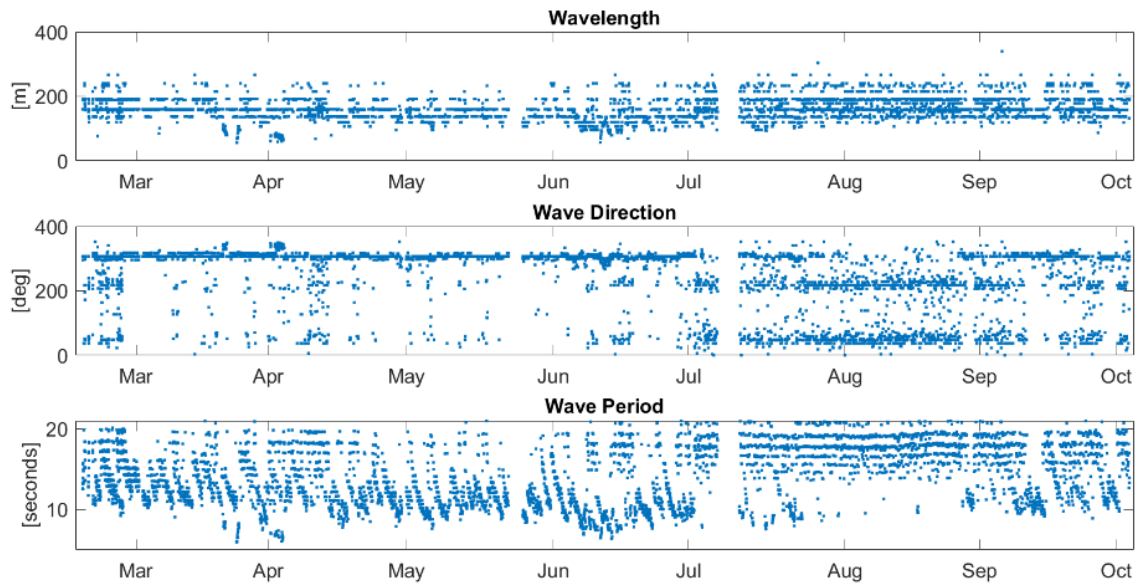


Figure 6. Wave parameters extracted from X-band radar data in NRT processing, during the Biarritz testing period. Note: data values shown are directly retrieved from the X-band radar and a validation and QC process is required to identify and discard (if needed) bad data.

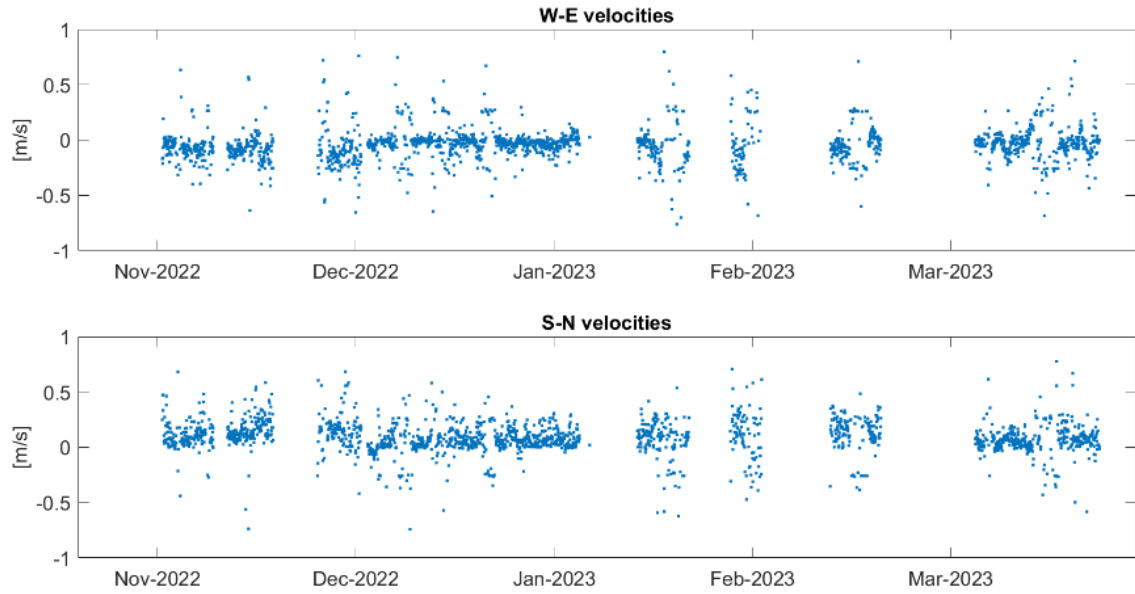


Figure 7. West-East and South-North currents extracted from X-band radar data in NRT processing, during the Bilbao testing period. Note: data values shown are directly retrieved from the X-band radar and a validation and QC process is required to identify and discard (if needed) bad data.

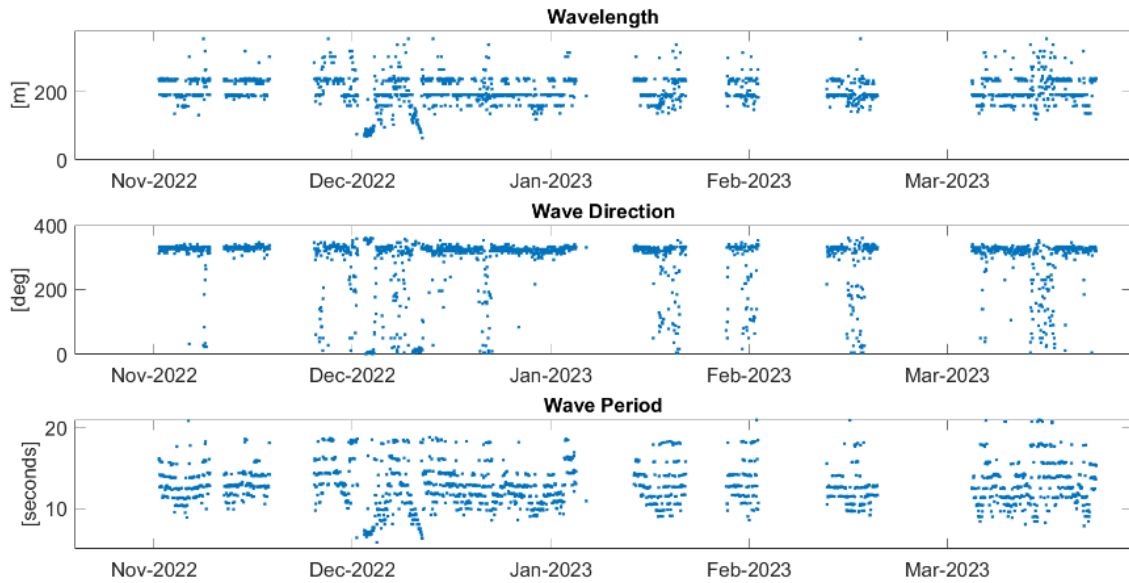


Figure 8. Wave parameters extracted from X-band radar data in NRT processing, during the Bilbao testing period. Note: data values shown are directly retrieved from the X-band radar and a validation and QC process is required to identify and discard (if needed) bad data.

4 Data QC, processing and validation

In order to validate the X-band radar data and establish quality references for the final data user, the output variables were compared to the in-situ installed ADCP variables in the Biarritz testing area (Figure 3). Comparing these remotely sensed measurements (X-band) with in-situ information (ADCPs) allows to assess the robustness of the former data.

The ADCPs used were Nortek Signature 500 kHz (ADCPs 1 and 2 in Figure 3) and Workhorse Sentinel 600 kHz (ADCPs 3 and 4 in Figure 3). The data from the 3rd ADCP were not exploitable, therefore ADCP 1, 2 and 4 were used. These calibrated ADCPs have a minimum accuracy of 0.3% of the observation ± 0.3 cm/s, thus providing accurate measurements.

Figure 9 shows an example of the visual comparison of surface currents from the X-band radar centred on the ADCP 4 location and data retrieved from ADCP 4, during March-April 2021. This figure also shows the Signal to Noise ratio (SNR) values, from X-band radar during the analysed period.

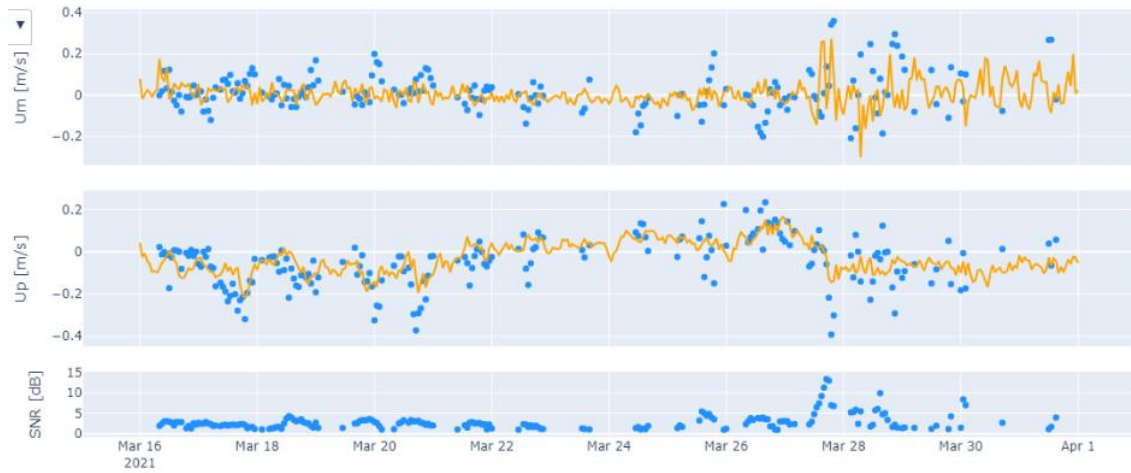


Figure 9. East-west (U_m) and north-south (U_p) surface current velocities comparison between X-band radar (blue dots) and ADCP (orange line) data and the corresponding SNR, from March 16 to April 1, 2021.

By analysing the distributions of the surface currents and of the SNR, it was concluded that non-expected high surface currents velocities were associated with SNR lower than 1 dB, which was linked to the limitations of the technology itself. Moreover, the comparison between X-band radar and ADCPs surface currents values indicated that surface currents higher than 0.6 m/s are not expected, as shown in figure 10.

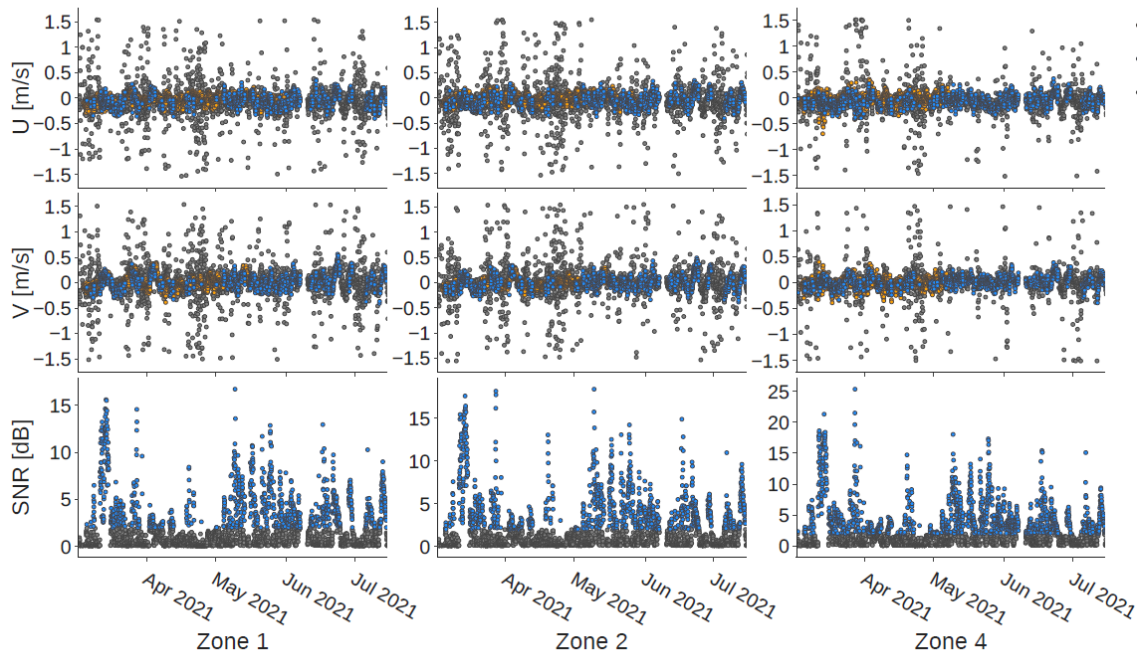


Figure 10. Example of East-west (U) and north-south (V) surface current velocities comparison between X-band radar good quality (blue dots) and discarded data (grey dots), together with ADCP (orange dots) data, together with SNR values from X-band radar from April to July 2021.

After the data comparison, 2 thresholds have been established to consider good data from this X-band radar instrument:

- $SNR > 1\text{dB}$
- $Velocity < 0.6\text{ m/s}$

As an example, after applying those two filters, the remaining data for the period March-May 2021 are represented together with the ADCP values in Figure 11.

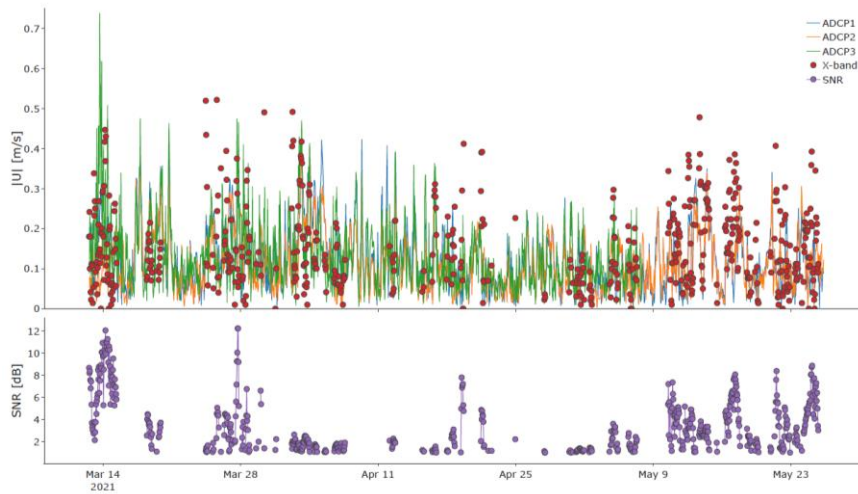


Figure 11. (up) X-band surface filtered and ADCP velocity module (down) SNR values.

Figure 12 shows the scatter plot applied to the whole X-band radar dataset, which shows the final correlation between X-band radar and ADCP values.

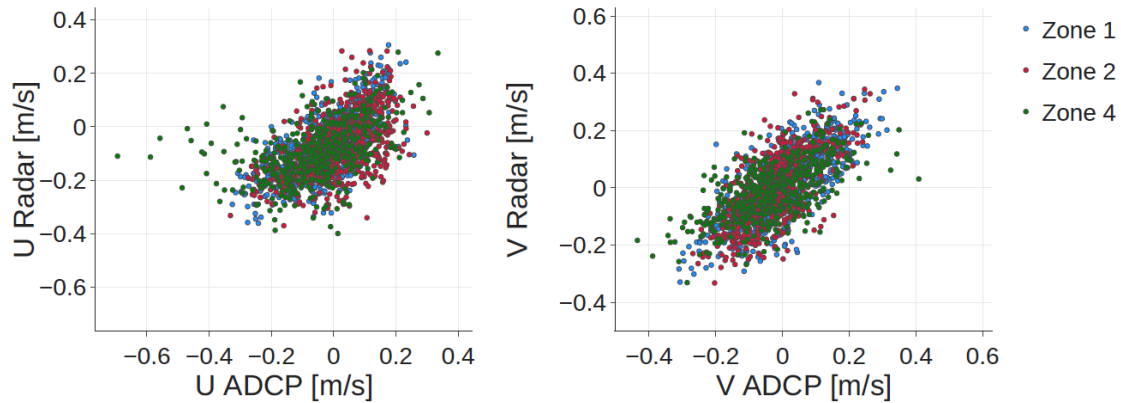


Figure 12. Scatter plot from X-band radar and ADCP velocity module values.

Finally, correlation and RMSE values have been summarized in Table 2:

Table 2. Correlation and RMSE values between X-band radar and ADCP values.

ZONE	1	2	4	ALL
RMSE U (m/s)	0.100	0.123	0.132	0.119
RMSE V (m/s)	0.086	0.088	0.093	0.089
Corr U	0.678	0.568	0.466	0.568
Corr V	0.754	0.703	0.649	0.700

Statistical comparison results show good agreement between in-situ and X-band radar values, taking into account that the study area is located in a coastal area, affected by tidal motions that rapidly change the direction of the surface currents. Moreover, the depth of both measurements though quite close, are not exactly the same.

5 Product description

The X-band radar datasets are created as individual NetCDF files. As a reference, the attributes listed herein correspond to the X-band radar data of Biarritz (the dataset of the Bilbao site contains the same attributes). Note that the datasets published in data repositories, due to the standards of these repositories, may contain minor differences in the global attributes. The general characteristics of these datasets are described in Table 3.

Table 3: General description of the X-band radar dataset of Biarritz.

Spatial Coverage	South-eastern Bay of Biscay
Spatial Resolution	Discrete
Temporal Coverage	From March 2021 to February 2022
Temporal Resolution	1 hour
Variables	Zonal and meridional water velocity and wave parameters; QC variables; and Metadata
File format	NetCDF

Dataset location	
Access to the dataset	Open access

Table 4 shows the variables that are embedded in the dataset, which compose the bulk of the dataset.

Table 4. Variables contained in the X-band radar dataset of Biarritz.

Variable name	Description	Units
DEPH	Depth of the measurement	m
EWCT	Meridional sea water velocity	m/s
LATITUDE	Latitude of the data position	Degrees North
LONGITUDE	Longitude of the data position	Degrees East
NSCT	Zonal sea water velocity	m/s
SNR	Signal-to-Noise Ratio	dB
TIME	Date of the data	Seconds since 1970-01-01T00:00:00z
VPED	Peak wave direction	Degrees
VTPK	Peak wave period	s
Wavelength	Peak wavelength	m

Table 5 provides much more information and details about the datasets and enables a deep understanding of them, contributing to making the datasets FAIR (Findable, Accessible, Interoperable, Reusable) (Tanhua et al., 2019). The proposed main and global attribute metadata followed the structures and standard names of the ‘NetCDF CF Metadata Convention Standard Name Table Version 1.6’ (<https://cfconventions.org/cf-conventions/v1.6.0/cf-conventions.html>). They also followed the ISOs 19115 and 19139, and several non-standard attributes. The Seadatanet common vocabularies were also used. The use of common standard metadata and vocabularies made the dataset more FAIR.

Table 5. Global attributes contained in the metadata of the X-band radar dataset of Biarritz.

Global attribute	Value
acknowledgment	‘These data were collected by SusTunTech project, processed by AZTI and made freely available by Marine Instruments through SusTunTech project and the programs that contribute to it’
area	‘South-eastern Bay of Biscay’
cdm_data_type	‘Point’
citation	‘These data were collected by SusTunTech project, processed by AZTI and made freely available by Marine Instruments through SusTunTech project and the programs that contribute to it’
comment	‘Currents and waves are derived from X-Band radar. Raw data were processed using ROWMS software and output data were quality controlled. The final product is a set of surface current velocities and wave parameters over a single longitude and latitude’
Contact	‘sustuntech_WP4@azti.es’
Conventions	‘ ‘
creator_email	‘sustuntech_WP4@azti.es’
creator_name	‘AZTI’
creator_type	‘Institution’
creator_url	‘ https://www.azti.es/ ’
data_assembly_center	‘AZTI, Marine Instruments’
data_language	‘eng’
data_mode	‘D’
data_type	‘Currents and waves’
date_update	‘2021-08-19 23:08’
distribution_statement	‘These data are public and free of charge. User assumes all risk for use of data. User must display citation in any publication or product using data. User must contact PI prior to any commercial use of data’
DOI	
format_version	‘1.4’

geospatial_lat_max	'-1.580278, -1.576944, -1.56944'
geospatial_lat_min	'-1.580278, -1.576944, -1.56944'
geospatial_lat_units	'degrees_north'
geospatial_lon_max	'43.495556, 43.498333, 43.496387'
geospatial_lon_min	'43.495556, 43.498333, 43.496387'
geospatial_lon_units	'degrees_east'
geospatial_vertical_max	'-1'
geospatial_vertical_min	'-1'
geospatial_vertical_units	'm'
history	'2021-03-16 05:09 - 2021-08-19 23:08 data collected. 2023-05-09 15:46 netCDF file created using Matlab software'
infoUrl	'https://www.sustuntech.eu/communicationmaterials/deliverables/'
institution	'AZTI (Spain)'
institution_edmo_code	'1623'
institution_references	'AZTI'
keywords	'OCEAN CURRENTS, OCEAN WAVES, FISHERIES'
keywords_vocabulary	'GCMD Science Keywords'
license	'X-band derived currents and waves dataset is licensed under a Creative Commons Attribution 4.0 International License. You should have received a copy of the license along with this work. If not, see http://creativecommons.org/licenses/by/4.0/ '
metadata_language	'eng'
naming_authority	'Marine Instruments, AZTI'
NetCDF_format	'netcdf4_classic'
NetCDF_version	'netCDF-4 classic model'
pi_name	' '
platform_code	' '
platform_name	' '
publisher_email	'sustuntech@globalmarine.es'
publisher_name	'Marine Instruments'
publisher_type	'Institution'
publisher_url	'https://www.marineinstruments.es/es/'
qc_manual	' '
references	'https://www.sustuntech.eu/, https://www.sustuntech.eu/communicationmaterials/deliverables/'
Standard_name_vocabulary	'NetCDF Climate and Forecast Metadata Convention Standard Name Table Version 1.6; and https://www.seadatanet.org/Standards/Common-Vocabularies '
summary	'Currents and waves are derived from X-Band radar. Raw data were processed using ROWMS software and output data were quality controlled. The final product is a set of surface current velocities and wave parameters over a single longitude and latitude'
time_coverage_end	2021-08-19 23:08
time_coverage_resolution	'1 hour'
time_coverage_start	2021-03-16 05:09
title	'Currents and wave parameters in the south-eastern Bay of Biscay by SusTunTech project'
update_interval	'void'
wmo_inst_type	' '
wmo_platform_code	' '

6 References

- Nieto Borge, J., Rodríguez, G. R., Hessner K., and González P. I. (2004). "Inversion of marine radar images for surface wave analysis," *Journal of Atmospheric and Oceanic Technology*, vol. 21, no. 8, pp. 1291–1300. doi: 10.1175/1520-0426(2004)021<1291:IOMRIF>2.0.CO;2.
- Seemann J., Carrasco R., Stresser M. (2017). "An operational wave monitoring system based on a Dopplerized marine radar", *OCEANS 2017 – Aberdeen*. doi:10.1109/OCEANSE.2017.8084814.
- Serafino, F., Lugni, C., and Soldovieri F. (2008). "Sea surface topography reconstruction from X-band radar images," en, *Advances in Geosciences*, vol. 19, pp. 83–86, issn: 1680-7359. doi: 10.5194/adgeo-19-83-2008. [Online]. Available: <https://adgeo.copernicus.org/articles/19/83/2008/> (visited on 02/16/2022).
- Tanhua T, Pouliquen S, Hausman J, O'Brien K, Bricher P, de Bruin T, Buck JJH, Burger EF, Carval T, Casey KS, Diggs S, Giorgetti A, Graves H, Harscoat V, Kinkade D, Muelbert JH, Novellino A, Pfeil B, Pulsifer PL, Van de Putte A, Robinson E, Schaap D, Smirnov A, Smith N, Snowden D, Spears T, Stall S, Tacoma M, Thijsse P, Tronstad S, Vandenberghe T, Wengren M, Wyborn L and Zhao Z (2019). "Ocean FAIR Data Services". *Front. Mar. Sci.* 6:440. 'DOI®': 10.3389/fmars.2019.00440.
- Valenzuela G. R. (1978). "Theories for the interaction of electromagnetic and oceanic waves—a review," *Boundary-Layer Meteorology*, vol. 13, no. 1, pp. 61–85. Doi:10.1007/BF00913863
- Young, I. R., Rosenthal, W., and Ziemer, F. (1985). "A three-dimensional analysis of marine radar images for the determination of ocean wave directionality and surface currents," *Journal of Geophysical Research*, vol. 90, no. C1, p. 1049, issn: 0148-0227. doi: 10.1029/JC090iC01p01049.